Research Paper

SUPCRTBL: A revised and extended thermodynamic dataset and software package of SUPCRT92

CrossMark

Kurt Zimmer [a,1], Yilun Zhang [b,1], Peng Lu [c,2], Yanyan Chen [c], Guanru Zhang [c], Mehmet Dalkilic [a], Chen Zhu [c,*]

[a] Computer Science, School of Informatics and Computing, Indiana University, Bloomington, IN 47405, USA
[b] Doctoral program in Environmental Sciences, Indiana University, Bloomington, IN 47405, USA
[c] Department of Geological Sciences, Indiana University, Bloomington, IN 47405, USA

ARTICLE INFO

ABSTRACT

The computer-enabled thermodynamic database associated with SUPCRT92 (Johnson et al., 1992) enables the calculation of the standard molal thermodynamic properties of minerals, gases, aqueous species, and reactions for a wide range of temperatures and pressures. However, new data on the thermodynamic properties of both aqueous species and minerals have become available since the database's initial release in 1992 and its subsequent updates. In light of these developments, we have expanded SUPCRT92's thermodynamic dataset and have modified the accompanying computer code for thermodynamic calculations by using newly available properties. The modifications in our new version include: (1) updating the standard state thermodynamic properties for mineral end-members with properties from Holland and Powell (2011) to improve the study of metamorphic petrology and economic geology; (2) adding As-acid, As-metal aqueous species, and As-bearing minerals to improve the study of environmental geology; (3) updating properties for Al-bearing species, $SiO_2^\circ(aq)$ and $HSiO_3^-$, boehmite, gibbsite, and dawsonite for modeling geological carbon sequestration. The new thermodynamic dataset and the modified SUPCRT92 program were implemented in a software package called SUPCRTBL, which is available online at www.indiana.edu/~hydrogeo/supcrtbl.html.

© 2016 Elsevier Ltd. All rights reserved.

1. Introduction

Oelkers et al. (2009) state that the creation of thermodynamic databases may be one of the past century's greatest advances in the field of geochemistry. These databases make it possible for quantitative interpretation and predication of geochemical systems. For example, the computer-enabled thermodynamic database affiliated with the computer program SUPCRT92 (Johnson et al., 1992) has greatly increased the efficiency of thermodynamic calculations. Furthermore, equilibrium constants generated from SUPCRT92 are basic input parameters for a variety of geochemical and reactive transport modeling codes (e.g., Toughreact, Phreeqc, Phast, EQ3/6, CHESS, CrunchFlow and HydroGeochem). These "higher order" codes have facilitated rapid chemical speciation, reaction path, and reactive mass transport simulations. The near 2000 citations of Johnson et al. (1992) are testimonial to the great

contribution of this work to the geological community.

The thermodynamic database embedded in SUPCRT92 is based on the compilation of a variety of thermodynamic datasets, extrapolations, and estimates reported by Helgeson and co-workers (Dale et al., 1997; Haas et al., 1995; Helgeson et al., 1978; Sassani and Shock, 1998; Schulte and Shock, 1993; Shock, 1992, 1993, 1995; Shock and Koretsky, 1993, 1995; Shock and McKinnon, 1993; Shock et al., 1997a; Sverjensky et al., 1997). The original SUPCRT92 database contains a limited number of minerals and aqueous species, whereas the applications of geochemical and reactive transport modeling for a variety of geological and environmental topics require a wide range of minerals and aqueous species. The database of SUPCRT92 has gone through a series of updates since its initial publication because of the need for a wider range of minerals and aqueous species. Some notable updates include sprons96.dat, slop98.dat, and slop07.dat (GEOPIG, 2010). Sprons96.dat included aqueous and mineral species relevant to the disposal of high-level nuclear wastes, while slop98.dat and slop07.dat focused on the addition of metal–organic complexes and other organic compounds.

The mineral data in these three updates have remained largely unchanged since 1992 (from Helgeson et al. (1978), i.e., HDNB). The HDNB database was one of the earliest and most widely used

internally consistent datasets of standard state thermodynamic properties for mineral end-members. The experimental data that it was based on, however, was mostly compiled before 1975; therefore, it is necessary to upgrade and expand the database by incorporating new data available on phase equilibrium constraints, calorimetry, and field data. Additionally, one major difference between the HDNB database and the newly upgraded and expanded database HP11 (Holland and Powell, 2011) is the treatment of the temperature and pressure dependence of mineral volumes. HDNB assumes mineral volumes are independent of temperature and pressure. It has since been recognized, however, that expansibilities and compressibilities can have significant effects on calculated Gibbs free energies of minerals (Berman, 1988; Holland et al., 1996; Pawley et al., 1996).

Currently, there is a tremendous amount of interest in arsenic geochemistry because of arsenic contamination in groundwater (Fukushi and Sverjensky, 2007; Lu and Zhu, 2011; Marini and Accornero, 2007, 2010; McKnight-Whitford et al., 2010; Nordstrom and Archer, 2002; Oremland and Stolz, 2003; Smedley and Kinniburgh, 2002; Sverjensky and Fukushi, 2006; Swartz et al., 2004). Significant discrepancies, nonetheless, still exist in the thermodynamic data for arsenic aqueous species and minerals in the literature. New values of thermodynamic properties for arsenic species have become available through several re-evaluations, compilations, estimations, or experiments (Langmuir et al., 2006; Marini and Accornero, 2007, 2010; Nordstrom and Archer, 2002; Pokrovski et al., 2002; Zhu et al., 2005). We have compiled the available data for the As–O–H–S–Fe–Ba system (Lu and Zhu, 2011) and incorporated them into our new thermodynamic database here.

In the last decade, a significant amount of research has focused on determining the feasibility of storing large amounts of CO_2 in deep geologic formations in order to reduce carbon dioxide emission into the atmosphere. Dissolution of the injected CO_2 will acidify the formation water and cause significant water–rock interactions that dissolve aluminosilicate minerals and precipitate carbonates (IPCC, 2005). In order to better simulating these reactions, we have updated the Al and Si-bearing aqueous and mineral species and some carbonate minerals in the new database.

2. Updates to the database

2.1. Updates for minerals of petrological interest

The variation of standard Gibbs free energy at any temperature and pressure can be computed by the equation (Anderson, 2008)

$$\Delta_a G^\circ_{T,P,i} = \Delta_f G^\circ_{T_r,P_r,i} + \int_{T_r}^{T} \left(\frac{\partial G_i^\circ}{\partial T} \right)_{P=P_r} dT + \int_{P_r}^{P} \left(\frac{\partial G_i^\circ}{\partial P} \right)_{T} dP \tag{1}$$

where $\Delta_a G^\circ_{T,P,i}$ refers to the apparent molar Gibbs free energy of formation from the elements of the subscripted substance i at the temperature T and the pressure P. $\Delta_f G^\circ_{T_r,P_r,i}$ denotes the standard molar Gibbs free energy of formation from the elements of the subscripted substance at the reference temperature T_r and pressure P_r. G_i° stands for the Gibbs free energy of the subscripted substance.

Integrating the second term and considering the relationship $\left(\frac{\partial G}{\partial P} \right)_T = V$, Eq. (1) becomes

$$\Delta_a G^\circ_{T,P,i} = \Delta_f G^\circ_{T_r,P_r,i} - S^\circ_{T_r,P_r,i}(T - T_r) + \int_{T_r}^{T} C_{Pi}^\circ dT - T \int_{T_r}^{T} C_{Pi}^\circ d \ln T$$
$$+ \int_{P_r}^{P} V_i^\circ dP \tag{2}$$

where $S^\circ_{T_r,P_r,i}$ refers to the standard molar entropy of the

subscripted substance at the reference temperature and pressure. C_{Pi}° and V_i° stand for the standard molar isobaric heat capacity and volume of the substance of interest, respectively.

Helgeson et al. (1978) indicated that mineral expansibilities and compressibilities in the Earth's crust are small because most minerals expand less than 3% with temperature increasing from 25 to 800 °C at 1 bar. Most minerals compress by less than 4% with increasing pressure from 1 bar to 40 kbars. Thus, past researchers have posited that the pressure and temperature effects on volume cancel out each other, and that mineral volumes can be approximated as being independent from temperature and pressure. Considering these assumptions, the last term of Eq. (2) becomes

$$\int_{P_r}^{P} V_i^\circ dP = V_i^\circ(P - 1) \tag{3}$$

Holland and Carpenter (1986), Holland et al. (1996) and Pawley et al. (1996), however, have argued that mineral expansibilities and compressibilities can have significant effects on calculated Gibbs free energies at high temperatures and pressures. Holland and Powell (2011) gave the G contribution by integrating V of the last term of Eq. (2):

$$\int_{P_r}^{P} V_i^\circ dP = PV_i^\circ \left(1 - a + \frac{a\left((1 - bP_{th})^{1-c} - (1 + b(P - P_{th}))^{1-c} \right)}{b(c - 1)P} \right) \tag{4}$$

with the relation of the parameters a, b and c to the bulk modulus and its derivatives at zero pressure (Freund and Ingalls, 1989):

$$a = \frac{1 + \kappa_0^`}{1 + \kappa_0^` + \kappa_0 \kappa_0^{``}},$$
$$b = \frac{\kappa_0^`}{\kappa_0} - \frac{\kappa_0^{``}}{1 + \kappa_0^`},$$
$$c = \frac{1 + \kappa_0^` + \kappa_0 \kappa^{``}}{\kappa_0^{`2} + \kappa_0^` - \kappa_0 \kappa_0^{``}}, \tag{5}$$

where κ_0 is the bulk modulus at 298.15 K and 1 bar, and κ_0' and κ_0'' are the first and second derivatives of κ_0. κ_0, κ_0' and κ_0'' have been provided by Holland and Powell (2011).

The thermal pressure term P_{th} can be expressed as (Holland and Powell, 2011):

$$P_{th} = \alpha_0 \kappa_0 \frac{\theta}{\xi_0} \left(\frac{1}{e^u - 1} - \frac{1}{e^{u_0} - 1} \right) \tag{6}$$

with $u = \theta/T$. Eq. (6) becomes

$$P_{th} = \alpha_0 \kappa_0 \frac{\theta}{\xi_0} \left(\frac{1}{e^{\frac{\theta}{T}} - 1} - \frac{1}{e^{\frac{\theta}{T_0}} - 1} \right) \tag{7}$$

where α_0 is the thermal expansion parameter, and

$$\xi_0 = \frac{u_0^2 e^{u_0}}{(e^{u_0} - 1)^2} = \frac{\left(\frac{\theta}{T_0} \right)^2 e^{\frac{\theta}{T_0}}}{\left(e^{\frac{\theta}{T_0}} - 1 \right)^2} \tag{8}$$

An empirical relationship for θ is derived for the substance of interest, $\theta_i = 10636/(S_i/n_i + 6.44)$, where S_i is the molar entropy (in $J\,K^{-1}\,mol^{-1}$) of i and n_i is the number of atoms in the chemical formula of i.

Different equations are used to represent the variation of mineral heat capacity with temperature, but there are no differences in principle. SUPCRT92 (Johnson et al., 1992) uses the Maier and Kelley (1932) equation,

$$C_p = a + bT + cT^{-2} \tag{9}$$

HP11, however, uses the heat capacity polynomial equation as

in HP98, which is

$$C_p = a + bT + cT^{-2} + dT^{-0.5} \qquad (10)$$

HP11 treated phase transition and order–disorder in minerals with the Landau model (for minerals listed in HP11 Table 2b) or Bragg–Williams type model (for minerals listed in HP11 Table 2c). We modified the SUPCRT92 codes to incorporate the Landau equations (see Appendix 1) and added Landau parameters into the database. However, for minerals listed in HP11 Table 2c, Holland and Powell (2011) did not give sufficient details for us to program the Bragg–Williams type model, but HP98 treated phase transition for some of these minerals with Landau model and the Landau model parameters were provided. Therefore, we used the Landau model and parameters for these minerals. Four minerals in Table 2c: Ca-Tschermaks pyroxene, sanidine, spinel, and hercynite have no Landau parameters in HP98 and picrochromite is new in HP11. Currently, these five minerals have no phase transition provisions in the SUPCRTBL package.

Fig. 1 compares the standard molal heat capacity, entropy, enthalpy, and Gibbs free energy of formation for quartz, calculated with the Landau model (SUPCRTBL) and with HDNB phase transition approach (SUPCRT92). The Landau model simulates the phase transition of quartz well. For $S_{T,P}^{\circ}$, $\Delta_f H_{T,P}^{\circ}$, $\Delta_f G_{T,P}^{\circ}$, the Landau model produces smooth curves at phase transition. Calculations using the Landau model for additional phases are shown in Appendix 1.

The $\Delta_f G_{T_r,P_r,i}^{\circ}$ values for minerals are needed to incorporate the HP11 dataset into our SUPCRTBL package, but they were not provided in HP11. We calculated $\Delta_f G_{T_r,P_r,i}^{\circ}$ values for each mineral with formation from the elements at 298.15 K and 1 bar, i.e. the Benson–Helgeson convention (Anderson, 2008). Standard molar entropy values for reference materials were taken from CODATA (Cox et al., 1989) when possible to ensure the internal consistency with other species in SUPCRTBL. For elements whose entropy values are

not available in CODATA (i.e., Fe and As), the entropy values were taken from Wagman et al. (1982). To verify the calculations, $\Delta_f G_{T_r,P_r,i}^{\circ}$ values for minerals in HP98 were calculated with the same reference materials and compared to published values. The differences were no more than rounding errors.

2.2. Updates for aqueous and mineral species of arsenic geochemistry

The interest in arsenic contamination in surface water and groundwater has greatly increased in recent years due to an increased concern for public health. Therefore, reliable thermodynamic data of arsenic is needed to perform speciation-solubility and sorption calculations in order to improve our understanding of geochemical controls over the mobility of arsenic (Welch et al., 2000). Unfortunately, as Nordstrom and Archer (2002) have pointed out, most previous compilations are unreliable. They further provided an internally consistent thermodynamic data set through simultaneous weighted least-squares multiple regressions on thermochemical measurements.

Thermodynamic data for ferric and ferrous bearing and barium bearing arsenate and arsenite species, however, are unavailable in their compilation. We compiled a set of internally consistent thermodynamic properties for arsenic, as described in Lu and Zhu (2011). These thermodynamic properties consist of those from Nordstrom and Archer (2002) (Note: Only 25 °C values are available and some only have $\Delta G_{f,T_r,P_r}^{\circ}$ values), metal arsenic complexes recalculated from Marini and Accornero (2010), amorphous ferric arsenate and scorodite recalculated from Langmuir et al. (2006), and barium arsenate and barium hydrogen arsenate recalculated from Zhu et al. (2005). The compilation of the new data for arsenic-bearing species is listed in Tables 1 and 2.
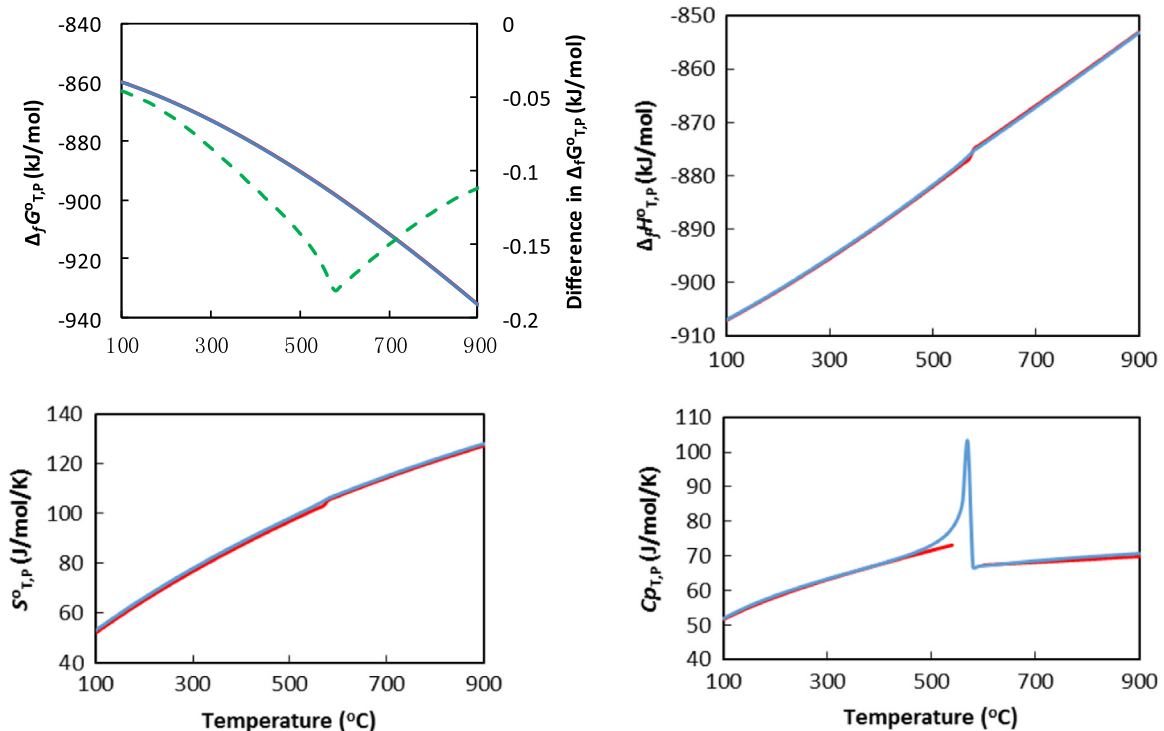

Fig. 1. Comparison of thermodynamic properties of quartz as a function of temperature at 1 bar between SUPCRTBL and SUPCRT92. SUPCRTBL (Blue lines) has better prediction of heat capacity lambda anomaly of quartz near its phase transition temperature than SUPCRT92 (Red lines). For $\Delta_f G_{T,P}^{\circ}$, the red and blue line overlap with each other (the difference is shown with green dashed line). The largest difference on $\Delta_f G_{T,P}^{\circ}$ occurs near the phase transition temperature, but all differences are small. (For interpretation of the references to color in this figure legend, the reader is referred to the web version of this article.)

Table 1
Thermodynamic properties for As-bearing aqueous species.

Species	$\Delta_f G^\circ_{Tr,Pr}$ (kJ/mol)	$\Delta_f H^\circ_{Tr,Pr}$ (kJ/mol)	$S^\circ_{Tr,Pr}$ (J/mol/K)	$C_{p,Tr,Pr}$ (J/mol/K)	$V^\circ_{Tr,Pr}$ (J/bar)	$a_1 \times 10$ (kJ/mol/ bar)	$a_2 \times 10^{-2}$ (kJ/mol)	a_3 (kJ/K/mol/bar)	$a_4 \times 10^{-4}$ (kJ/K/mol)	c_1 (kJ/mol/ K)	$c_2 \times 10^{-4}$ (kJ K/mol)	$\omega \times 10^{-5}$ (kJ/mol)	Ref.
$H_3AsO_4^\circ$	− 766.75	− 903.45	183.05										1
$H_2AsO_4^-$	− 753.65	− 911.42	112.38										1
$H_2AsO_4^{2-}$	− 713.73	− 908.41	− 11.42										1
AsO_4^{3-}	− 646.36	− 890.21	− 176.31										1
$H_3AsO_3^\circ$	− 639.80	− 742.36	195.81										1
$H_2AsO_3^-$	− 587.66	− 714.74	112.80										1
$HAsO_3^{2-}$	− 507.40												1
AsO_3^{3-}	− 421.80												1
$As_3S_4(HS)_2^-$	− 125.60												1
$AsS(OH)SH^-$	− 244.40												1
$NaH_2AsO_4^\circ$	− 1004.91	− 1140.59	172.38	158.16	4.11	0.03087	0.04282	0.00478	− 0.01340	0.11682	0.01951	− 0.00016	2
$KH_2AsO_4^\circ$	− 1024.81	− 1147.89	228.03	91.63	5.24	0.03735	0.05867	− 0.00203	− 0.01405	0.07787	0.00593	− 0.00016	2
$MgH_2AsO_4^+$	− 1217.17	− 1392.09	− 43.51	212.13	1.83	0.01887	0.01353	0.01736	− 0.01219	0.17684	0.03050	0.00293	2
$CaH_2AsO_4^+$	− 1314.49	− 1456.06	77.40	191.63	2.22	0.02048	0.01746	0.01567	− 0.01235	0.14794	0.02630	0.00110	2
$SrH_2AsO_4^+$	− 1321.71	− 1455.37	114.22	167.78	2.29	0.02071	0.01801	0.01543	− 0.01237	0.12893	0.02147	0.00054	2
$MnH_2AsO_4^+$	− 989.44	− 1133.14	60.67	223.84	2.33	0.02118	0.01916	0.01494	− 0.01242	0.16914	0.03288	0.00136	2
$FeH_2AsO_4^+$	− 860.62	− 1019.72	4.18	187.86	1.76	0.01821	0.01192	0.01805	− 0.01212	0.15610	0.02559	0.00221	2
$CoH_2AsO_4^+$	− 809.14	− 972.18	− 6.28	189.12	1.39	0.01616	0.00691	0.02020	− 0.01191	0.15812	0.02578	0.00237	2
$NiH_2AsO_4^+$	− 808.12	− 978.16	− 29.71	152.30	1.00	0.01405	0.00175	0.02241	− 0.01170	0.13995	0.01831	0.00273	2
$CuH_2AsO_4^+$	− 698.17	− 855.13	17.15	208.78	1.49	0.01662	0.00802	0.01972	− 0.01196	0.16639	0.02981	0.00201	2
$ZnH_2AsO_4^+$	− 903.44	− 1068.48	− 1.26	212.13	1.53	0.01690	0.00872	0.01942	− 0.01199	0.17102	0.03052	0.00229	2
$PbH_2AsO_4^+$	− 786.16	− 901.97	187.02	142.67	2.50	0.02149	0.01992	0.01461	− 0.01245	0.10422	0.01639	− 0.00056	2
$AlH_2AsO_4^{2+}$	− 1255.11	− 1467.40	− 238.49	146.02	− 0.71	0.00606	− 0.01776	0.03079	− 0.01089	0.18636	0.01703	0.00816	2
$FeH_2AsO_4^{2+}$	− 794.75	− 985.48	− 166.94	276.98	0.11	0.01042	− 0.00712	0.02622	− 0.01133	0.25287	0.04368	0.00708	2
$NaHAsO_4^-$	− 979.16	− 1141.97	81.17	46.02	1.64	0.01868	0.01305	0.01756	− 0.01217	0.10401	− 0.00331	0.00555	2
$KHAsO_4^-$	− 998.95	− 1151.63	128.45	16.32	2.61	0.02397	0.02597	0.01201	− 0.01270	0.08010	− 0.00934	0.00484	2
$MgHAsO_4^\circ$	− 1182.63	− 1365.89	− 71.55	− 14.23	− 0.05	0.00706	− 0.01531	0.02974	− 0.01099	0.01618	− 0.01558	− 0.00016	2
$CaHAsO_4^\circ$	− 1280.46	− 1440.72	14.64	− 23.43	0.20	0.00846	− 0.01189	0.02827	− 0.01114	0.01083	− 0.01744	− 0.00016	2
$SrHAsO_4^\circ$	− 1287.63	− 1443.13	41.00	− 33.89	0.24	0.00872	− 0.01126	0.02800	− 0.01116	0.00467	− 0.01959	− 0.00016	2
$MnHAsO_4^\circ$	− 960.50	− 1121.45	2.93	− 8.79	0.27	0.00885	− 0.01095	0.02787	− 0.01117	0.01921	− 0.01452	− 0.00016	2
$FeHAsO_4^\circ$	− 824.08	− 995.62	− 37.24	− 24.69	− 0.09	0.00680	− 0.01595	0.03001	− 0.01097	0.00992	− 0.01776	− 0.00016	2
$CoHAsO_4^\circ$	− 784.57	− 959.14	− 44.77	− 24.27	− 0.32	0.00548	− 0.01918	0.03140	− 0.01083	0.01017	− 0.01767	− 0.00016	2
$NiHAsO_4^\circ$	− 774.39	− 953.93	− 61.50	− 40.58	− 0.57	0.00408	− 0.02260	0.03287	− 0.01069	0.00063	− 0.02100	− 0.00016	2
$CuHAsO_4^\circ$	− 669.62	− 840.13	− 28.03	− 15.48	− 0.26	0.00584	− 0.01830	0.03102	− 0.01087	0.01530	− 0.01588	− 0.00016	2
$ZnHAsO_4^\circ$	− 877.92	− 1054.90	− 41.42	− 14.23	− 0.24	0.00596	− 0.01800	0.03089	− 0.01088	0.01621	− 0.01557	− 0.00016	2
$PbHAsO_4^\circ$	− 753.62	− 897.51	92.88	− 44.77	0.37	0.00945	− 0.00949	0.02724	− 0.01124	− 0.00181	− 0.02185	− 0.00016	2
$AlHAsO_4^+$	− 1237.98	− 1436.69	− 192.88	− 156.06	− 0.82	0.00442	− 0.02176	0.03251	− 0.01073	− 0.01741	− 0.04449	0.00520	2
$FeHAsO_4^+$	− 787.38	− 971.57	− 145.18	− 97.93	− 0.49	0.00609	− 0.01770	0.03076	− 0.01090	0.00992	− 0.03264	0.00447	2
$NaAsO_4^{2-}$	− 935.96	− 1062.50	202.92	− 160.67	− 1.70	0.00118	− 0.02968	0.03591	− 0.01040	0.02863	− 0.04546	0.01050	2
$KAsO_4^{2-}$	− 955.74	− 1042.02	351.46	− 190.37	− 0.96	0.00465	− 0.02120	0.03227	− 0.01075	− 0.00938	− 0.05149	0.00825	2
$MgAsO_4^-$	− 1135.85	− 1285.81	40.33	− 230.12	− 2.60	− 0.00540	− 0.04576	0.04281	− 0.00974	− 0.05159	− 0.05954	0.00617	2
$CaAsO_4^-$	− 1233.92	− 1351.91	156.48	− 239.32	− 2.55	− 0.00572	− 0.04654	0.04315	− 0.00970	− 0.07315	− 0.06141	0.00441	2
$SrAsO_4^-$	− 1239.48	− 1352.43	183.68	− 249.78	− 2.54	− 0.00581	− 0.04676	0.04324	− 0.00969	− 0.08312	− 0.06356	0.00400	2

MnAsO$_4^-$	−913.32	−1036.82	128.45	−224.68	−2.54	−0.00551	−0.04601	0.04292	−0.00973	−0.06085	−0.05849	0.00484	2
FeAsO$_4^-$	−781.02	−914.38	90.79	−240.58	−2.61	−0.00571	−0.04652	0.04314	−0.00970	−0.06487	−0.06172	0.00541	2
CoAsO$_4^-$	−741.36	−880.65	73.64	−240.16	−2.65	−0.00589	−0.04695	0.04332	−0.00969	−0.06223	−0.06164	0.00567	2
NiAsO$_4^-$	−737.66	−884.16	49.37	−256.48	−2.70	−0.00604	−0.04731	0.04348	−0.00967	−0.06837	−0.06496	0.00604	2
CuAsO$_4^-$	−634.89	−768.21	96.65	−231.38	−2.64	−0.00593	−0.04705	0.04337	−0.00968	−0.06032	−0.05985	0.00532	2
ZnAsO$_4^-$	−837.31	−978.44	79.08	−230.12	−2.64	−0.00582	−0.04678	0.04325	−0.00969	−0.05695	−0.05953	0.00559	2
PbAsO$_4^-$	−710.41	−813.52	229.70	−260.66	−2.52	−0.00590	−0.04698	0.04334	−0.00969	−0.09599	−0.06582	0.00331	2
AlAsO$_4^\circ$	−1194.77	−1380.77	−150.21	−251.88	−0.98	0.00175	−0.02829	0.03531	−0.01046	−0.12277	−0.06402	−0.00016	2
FeAsO$_4^\circ$	−744.17	−914.40	−98.32	−354.80	−1.31	−0.00016	−0.03296	0.03732	−0.01026	−0.18291	−0.08499	−0.00016	2
NaH$_2$AsO$_3^\circ$	−850.48	−957.43	166.10	118.83	3.27	0.02604	0.03104	0.00984	−0.01291	0.09386	0.01150	−0.00016	2
AgH$_2$AsO$_3^\circ$	−516.83	−615.35	185.35	107.95	3.30	0.02624	0.03152	0.00963	−0.01293	0.08748	0.00928	−0.00016	2
MgH$_2$AsO$_3^+$	−1051.90	−1197.39	−47.28	172.80	0.99	0.01407	0.00179	0.02240	−0.01170	0.15442	0.02250	0.00299	2
CaH$_2$AsO$_3^+$	−1150.27	−1263.03	71.55	152.30	1.38	0.01568	0.00574	0.02070	−0.01186	0.12582	0.01830	0.00119	2
SrH$_2$AsO$_3^+$	−1153.11	−1258.14	107.95	128.45	1.45	0.01591	0.00630	0.02046	−0.01189	0.10688	0.01347	0.00064	2
BaH$_2$AsO$_3^+$	−1156.10	−1246.56	167.78	107.11	1.99	0.01867	0.01305	0.01756	−0.01217	0.08616	0.00915	−0.00026	2
CuH$_2$AsO$_3^+$	−562.20	−690.04	12.55	169.45	0.65	0.01181	−0.00371	0.02476	−0.01147	0.14412	0.02181	0.00209	2
PbH$_2$AsO$_3^+$	−640.73	−728.28	179.08	103.34	1.65	0.01670	0.00823	0.01963	−0.01197	0.08235	0.00838	−0.00044	2
AlH$_2$AsO$_3^+$	−1115.50	−1295.42	−232.21	106.69	−1.56	0.00121	−0.02962	0.03588	−0.01040	0.16257	0.00902	0.00807	2
FeH$_2$AsO$_3^+$	−645.98	−805.06	−163.59	237.65	−0.73	0.00557	−0.01895	0.03130	−0.01084	0.22941	0.03568	0.00703	2

[1]Nordstrom and Archer (2002).
[2]Marini and Accornero (2010).

Table 2
Thermodynamic properties for As-bearing solids.

Species	$\Delta_f G^\circ_{Tr,Pr}$ (kJ/mol)	$\Delta_f H^\circ_{Tr,Pr}$ (kJ/mol)	$S^\circ_{Tr,Pr}$ (J/mol/ K)	Ref.
As(α)	0	0	35.63	1
As$_2$O$_3$(Arsenolite)	-576.34	-657.27	107.38	1
As$_2$O$_3$(Claudetite)	-576.53	-655.67	113.37	1
As$_2$O$_5$	-774.76	-917.59	105.44	1
AsS(α-Realgar)	-31.30	-31.80	62.90	1
AsS(β, Realgar)	-30.90	-31.00	63.50	1
As$_2$S$_3$(Orpiment)	-84.90	-85.80	163.80	1
As$_2$S$_3$(Orpiment, am)	-76.80	-66.90	200.00	1
FeAsS(Arsenopyrite)	-141.60			2
FeAsO$_4$:2H$_2$O(Scorodite)	-1287.08			3
FeAsO$_4$:2H$_2$O(Ferric–As,am)	-1270.98			3
Ba$_3$(AsO$_4$)$_2$(Barium–As)	-3095.11			4
BaHAsO$_4$:H$_2$O(Barium–H–As)	-1538.65			4

[1]Nordstrom and Archer (2002), [2]Ball and Nordstrom (1991),
[3]Langmuir et al. (2006), [4]Zhu et al. (2005).

3. Updates for aqueous and mineral species in the interest of geological carbon sequestration

The injection of CO$_2$ into deep saline aquifers is being considered as an option for greenhouse gas mitigation (IPCC, 2005). Four trapping mechanisms have been identified for the underground storage of CO$_2$: (1) structural and stratigraphic trapping; (2) residual CO$_2$ trapping; (3) solubility trapping; and (4) mineral trapping (Bachu, 2008; IPCC, 2005). Reactive transport modeling (RTM) has been used to model the geochemical interactions of CO$_2$-brine-host rock in order to understand the storage process, which is instrumental for evaluating the capacity and safety of the reservoir, and the fate of the injected CO$_2$ (Andre et al., 2007; Johnson et al., 2004; Liu et al., 2011; Strazisar et al., 2006; Xu et al., 2004; Zhang et al., 2015; Zhu et al., 2015). It is has been previously noted that the quality of the thermodynamic database used in the RTM contributes significantly to the inherent uncertainties in the modeling approach (IPCC, 2005). We have updated Al-bearing species, SiO$_2^\circ$ and HSiO$_3^-$, boehmite and gibbsite to improve the modeling of aluminosilicate reactions and dawsonite for the mineral carbonation.

Thermodynamic properties for aqueous Al species (Al^{3+}, Al(OH)$_2^+$, AlOH^{2+}, Al(OH)$_4^-$, Al(OH)$_3$(aq), NaAl(OH)$_4$(aq), AlH$_3$SiO$_4^{2+}$) have been evaluated and discussed in Zhu and Lu (2009). We adopted the properties from Tagirov and Schott (2001). It should be mentioned that the thermodynamic properties for Al-bearing species in sprons96.dat are from Pokrovskii and Helgeson (1995) while those in slop98.dat and slop07.dat are from Shock et al. (1997b). Data in Pokrovskii and Helgeson (1995) yield predictions of boehmite solubility at 250–350 °C in weakly acid and near-neutral solutions ∼1.5 order of magnitude higher than experimental results and this inconsistency increases with temperature (Tagirov and Schott, 2001).

Thermodynamic properties of species SiO$_2^\circ$(aq) in the earlier versions of SUPCRT92 are from Shock et al. (1997b). These
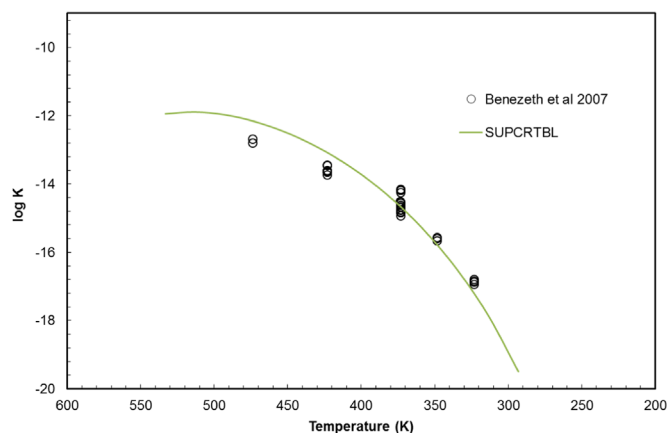

Fig. 2. Log K's of dawsonite reaction Eq. (11) as a function of temperature. Symbols stand for the solubility data in Benezeth et al. (2007). The line denotes calculation result of SUPCRTBL with derived $\Delta_f G^\circ_{Tr,Pr}$ value.

properties have long been somewhat controversial, especially at temperatures near 25 °C (Tutolo et al., 2014). Rimstidt (1997) performed a new set of quartz solubility experiments in the range of 21–96 °C, the duration of which were up to 4917 days. These experiments yielded quartz solubility that are higher than earlier studies, and were selected by Apps and Spycher (2004) and by Gunnarsson and Arnórsson (2000) for re-evaluation standard state partial molal properties for SiO$_2^\circ$(aq) and H$_4$SiO$_4^\circ$(aq), respectively. In the SUPCRTBL database, we retained the values for SiO$_2^\circ$(aq) from Apps and Spycher (2004) and also those for H$_4$SiO$_4^\circ$(aq) from Stefansson (2001). Stefansson (2001) derived standard molal properties for H$_4$SiO$_4^\circ$(aq) from quartz and amorphous solubility data by using the Gibbs free energy data for quartz from HDNB. HP11 and HDNB practically use the same value of $\Delta_f G^\circ_{Tr,Pr}$ for quartz (-856.24 and -856.28 kJ/mol, respectively). Therefore, we consider the quartz and aqueous silica values are consistent. Thermodynamic properties of HSiO$_3^-$ were then calculated taking account of the change of the properties of SiO$_2^\circ$(aq), using the difference in Shock et al. (1997b).

The only aluminum oxyhydroxide mineral listed in the Holland and Powell (2011) database is diaspore, because it is the stable phase at the T, P of petrological interest. Boehmite and gibbsite, however, are two other common minerals often found in experiments and in nature at lower temperatures. Therefore, their thermodynamic properties need to be added into the new database. We adopted the heat capacity, entropy, and enthalpy of formation for boehmite from Hemingway et al. (1991). We also examined the consistency of these thermodynamic properties with the rest of Holland and Powell (2011) carefully following the method of Zhu and Lu (2009). C_p data was fitted to the Holland and Powell C_p function ($C_p = a + bT + cT^{-2} + dT^{-0.5}$).

For gibbsite, we followed the same procedure as boehmite. To date, most gibbsite solubility data in the literature has been calculated based on the thermodynamic properties from Robie et al.

Table 3
Standard state properties of the aqueous species involved in Eq. (11) in SUPCRTBL database and the thermodynamic properties for dawsonite.

	Na$^+$	Al(OH)$_4^-$	HCO$_3^-$	H$_2$O	[a]Dawsonite in this study	Dawsonite in Benezeth et al. (2007)
[b]$\Delta_f G^\circ_{Tr,Pr}$	-261.881	-1305.772	-586.94	-237.183	-1782.3	-1782 ± 2
[b]$\Delta_f H^\circ_{Tr,Pr}$	-240.3	-1483.575	-689.933	-285.838	-1939.1	-1964 ± 7
[c]$S^\circ_{Tr,Pr}$	58.409	103.5456	98.449	69.923	137.7	132 ± 2

[a] $\Delta_f G^\circ_{Tr,Pr}$(dawsonite)$= \Delta_f G^\circ_{Tr,Pr}$(Al(OH)$_4^-$)$+ \Delta_f G^\circ_{Tr,Pr}$(HCO$_3^-$)$+ \Delta_f G^\circ_{Tr,Pr}$(Na$^+$)$- 2 \times \Delta_f G^\circ_{Tr,Pr}$(H$_2$O)$- \Delta G^\circ_{r,Tr,Pr}$. The calculations of $\Delta_f H^\circ_{Tr,Pr}$ and $S^\circ_{Tr,Pr}$ are the same.
[b] In kJ/mol.
[c] In kJ/mol/K.

(a)

```
FORSTERITE          Mg2SiO4
fo                  Mg(2)Si(1)O(4)
HP11                30.MAY.14
        -2053.50        -2172.57        95.10           4.366
        0.2333          0.1494          -603.80         -1.8697
        2.85            1285.0          3.84            -0.0030     7.000
        9999.0
```

Mineral name	Chemical formula			
Mineral abbreviation	Chemical stoichiometry			
Database	Date last modified			
$\Delta_f G^o{}_{Tr,Pr}$ (kJ/mol)	$\Delta_f H^o{}_{Tr,Pr}$ (kJ/mol)	$S^o{}_{Tr,Pr}$ (J/mol/K)	$V^o{}_{Tr,Pr}$ (J/bar)	
a (kJ/mol/K)	b (10^5 kJ/mol/K^2)	c (kJ·K/mol)	d (kJ/mol/K$^{-0.5}$)	
α_0 (10^5 K^{-1})	κ_0 (kbar)	κ'_0 (1)	κ''_0 (kbar^{-1})	Number of atoms in chemical formula
T_{max}				

(b)

```
QUARTZ              SiO2
q                   Si(1)O(2)
HP11                30.MAY.14
        -856.28         -910.70         41.43           2.269
        0.0929          -0.0642         -714.90         -0.7161
        0.00            730.0           6.00            -0.0082     3.000
        847.00          4.95            0.1188
        9999.0
```

Mineral name	Chemical formula			
Mineral abbreviation	Chemical stoichiometry			
Database	Date last modified			
$\Delta_f G^o{}_{Tr,Pr}$ (kJ/mol)	$\Delta_f H^o{}_{Tr,Pr}$ (kJ/mol)	$S^o{}_{Tr,Pr}$ (J/mol/K)	$V^o{}_{Tr,Pr}$ (J/bar)	
a (kJ/mol/K)	b (10^5 kJ/mol/K^2)	c (kJ·K/mol)	d (kJ/mol/K$^{-0.5}$)	
α_0 (10^5 K^{-1})	κ_0 (kbar)	κ'_0 (1)	κ''_0 (kbar^{-1})	Number of atoms in chemical formula
T_C° (K)	S_{max} (J/mol/K)	V_{max} (J/bar)		
T_{max}				

Fig. 3. The generic species block for minerals in spronsbl.dat. (a) Minerals that do not undergo phase transitions. Data for forsterite are used here as an example. (b) Minerals that undergo phase transitions. Landau model parameters from HP11 and HP98 are added for calculating phase transitions. T_{max} is the upper limit of the heat capacity parameters left over from SUPCRT92. Because HP11 does not give the upper limit for individual minerals, we set a default value of 9999 K. Users are responsible for minding the upper limits by themselves. T_C°, S_{max}, and V_{max} denote critical temperature at 1 bar, entropy and volume of disordering at T_C°, respectively. All other symbols in the figure are defined in preceding text.

(1978), which are based on heat of dissolution and heat capacity measurements reported in Hemingway et al. (1977,·1978). Gibbsite data in Tagirov and Schott (2001), for example, is from Robie et al. (1978), with the heat capacity given in Wesolowski (1992). The data in Robie et al. (1978) is cited by Robie and Hemingway (1995) and the source of the data in Wesolowski (1992) is Hemingway

```
471         Cp   = a  +  b*T  +  c/T**2  +  d/T**.5

491         CpdT  = a*(T2   -   T1)  +  b/2.0d0  *(T2 ** 2  -  T1 ** 2)  -
492       2         c*( 1.0d0  /T2  -   1.0d0  /T1) +
493       3         d/0.5d0  *(T2 ** .5   -  T1 ** .5 )

51 1        CpdlnT  = a*DLOG(T2 /T1)  +  b*(T2   -   T1)  -
512       2         c/2.0d0  *( 1.0d0  /T2 ** 2  -  1.0d0  /T1 ** 2) -
513       3         d/0.5d0  *( 1.0d0  /T2 ** 0.5 - 1.0d0  /T1 ** 0.5 )
```

Fig. 4. Updated piece of code for the heat capacity in C_p, C_pdT, $C_p$dlnT, respectively.

```
317    a = (1 + KappaP(i))
318 1    /(1 + KappaP(i) + Kappa(i)*KappaDP(i))
319    b = (KappaP(i)/Kappa(i)) -
320 1    (KappaDP(i)/(1 + KappaP(i)))
321    c = (1 + KappaP(i) + Kappa(i)*KappaDP(i))/
322 1       (KappaP(i)*(1+KappaP(i)) - Kappa(i)*KappaDP(i))
323    Theta = 10636/((SPrTrm(i)*4.184)/NumAtoms(i) + 6.44)
324    Eps = ((Theta/T0)**2)*EXP(Theta/T0)/((EXP(Theta/T0) - 1)**2)
325    Pth = Alpha(i)*Kappa(i)*(Theta/(Eps))*
326 1       (1/(EXP(Theta/(T)) - 1) - 1/(EXP(Theta/T0) - 1))

377    VdP = Vmin * ( P *(1 - a) + a * ((1 - b * Pth)**(1-c) -
378 1           (1 + b * (P - Pth))**(1-c)) / (b * (c - 1)))
379    VdP = VdP*100/4.184
380    Vmin = Vmin*(1 - a*(1 - (1 + b*(P/1000
381 1       - Pth))**(-1.0 * c)))
```

Fig. 5. Updated piece of code for the new volume contribution.

et al. (1977). Therefore, we adopted the thermodynamic properties from Robie et al. (1978), and then conducted non-linear fitting of C_p data to the Holland and Powell C_p function ($C_p = a + bT + cT^{-2} + dT^{-0.5}$). The Holland and Powell coefficients (a, b (10^5), c and d) are 0.092797, 18.943789, 133.865406 and -1.034267 (in kJ, mol and K), respectively.

A considerable amount of RTM modeling results indicate that the injection of CO_2 into deep sedimentary formations will lead to the formation of various carbonate minerals, including dawsonite. The thermodynamic properties for dawsonite, however, are limited and this is indicative of considerable obstacles for CO_2 sequestration modeling. The thermodynamic properties of dawsonite were derived from previous experimental measurements in the present study in order to reduce the uncertainty during the modeling.

Ferrante et al. (1976) determined the thermodynamic properties of synthetic dawsonite from a series of calorimetric studies. Employing the heat capacities determined from 6 to 307 K in their study, the C_p coefficients of dawsonite were derived according to the Holland–Powell C_p equation (i.e., $C_p = a + bT + cT^{-2} + dT^{-0.5}$) by least-squares regression. The resulted Holland and Powell C_p coefficients (a, b (10^5), c and d) are 0.009553, 48.643184, 1.062736, and -0.088676 (in kJ, mol and K), respectively. Recently, Benezeth et al. (2007) measured the solubility of synthetic dawsonite according to the equilibrium:

$$NaAlCO_3(OH)_2 + 2H_2O = Al(OH)_4^- + HCO_3^- + Na^+ + H^+ \qquad (11)$$
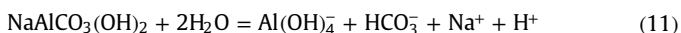
at 50–200 °C. Additionally, $\Delta G_{r,Tr,Pr}^\circ$, $\Delta H_{r,Tr,Pr}^\circ$ and $S_{r,Tr,Pr}^\circ$ were calculated in their study, which were 102.1 kJ/mol, 97.0 kJ/mol, and -17.1 kJ/mol/K, respectively. Combining the reported ΔG_r°, ΔH_r° and S_r° values, with the thermodynamic properties of $Al(OH)_4^-$, HCO_3^-, Na^+ and H_2O in SUPCRTBL database, we were able to derive a set of $\Delta_f G_{Tr,Pr}^\circ$, $\Delta_f H_{Tr,Pr}^\circ$, $S_{Tr,Pr}^\circ$ for dawsonite that are internally consistent with our own database (Table 3). As seen in Table 2, the retrieved $\Delta_f G_{Tr,Pr}^\circ$ value was similar to the data derived in Benezeth et al. (2007). The SUPCRTBL calculations with derived thermodynamic data can fit the laboratory measurements fairly well (Fig. 2).

4. Updates of the SUPCRT92 code

We made four major modifications to the source code of SUPCRT92. The first modification was to implement the heat capacity polynomial equations and volume function from Holland and Powell (2011) into the code. The code of CPRONS92 was modified to take into account the updated format of the database and re-named into CPRONSBL (see Supplement material for the exact line by line list of major modifications). CPRONS92 is the program that converts the code of a sequential access file to a direct access file that SUPCRT92 can read. The update to the database included six new properties for each mineral: d (the fourth heat capacity variable), α, κ_0, κ_0', κ_0'' and the number of atoms in its chemical formula. Fig. 3 shows an example of updated data block of forsterite. Likewise, the maximum size of the input sequential access file was increased from 10,000 lines to 1,000,000 lines to accommodate the expansion in size of the input file.

Second, the code of SUPCRT92 was modified in three different files, REAC_BL.for, REP_BL.for, and SUPCRTBL.for (see Supplement material for the exact line by line list of major modifications). In all of these files, the maximum amount of reaction parameter was adjusted from 50 to 3000 and the maximum increments for uniform and non-uniform tables was reduced from 75 to 21 in order to facilitate the database generation by batch calculations. To update the heat capacity equations, the code in the procedures Cptrms, Cp, CpdT, $C_p$dlnT in REAC_BL.for were also changed (Fig. 4).

For the changes to the mineral volume equations, only the Vterms procedure in REAC_BL.for was modified with the new volume contribution to the Gibbs free energy equation (Fig. 5).

Third, the HP11 dataset has a drastically different approach from HDNB to calculate thermodynamic properties related to phase transition and order–disorder. SUPCRT92 divided minerals according to the number of phase transitions, and different heat capacity functions for phases above and below the temperature of phase transition are used. HP11 uses the Landau theory approach, which was programmed into SUPCRTBL. The details are given in Appendix 1.

The fourth major change is that we no longer use calories and have adopted joules for all properties in the database and output files. The rest of the changes made to SUPCRT92 were to enable the reading of the new database into the data structures and variables used by the program.

5. Example calculations

Rimstidt (1997) conducted quartz dissolution experiments at temperatures from 21 to 96 °C, evaluated quartz solubility data in literature at temperature from 0 to 370 °C, and determined the
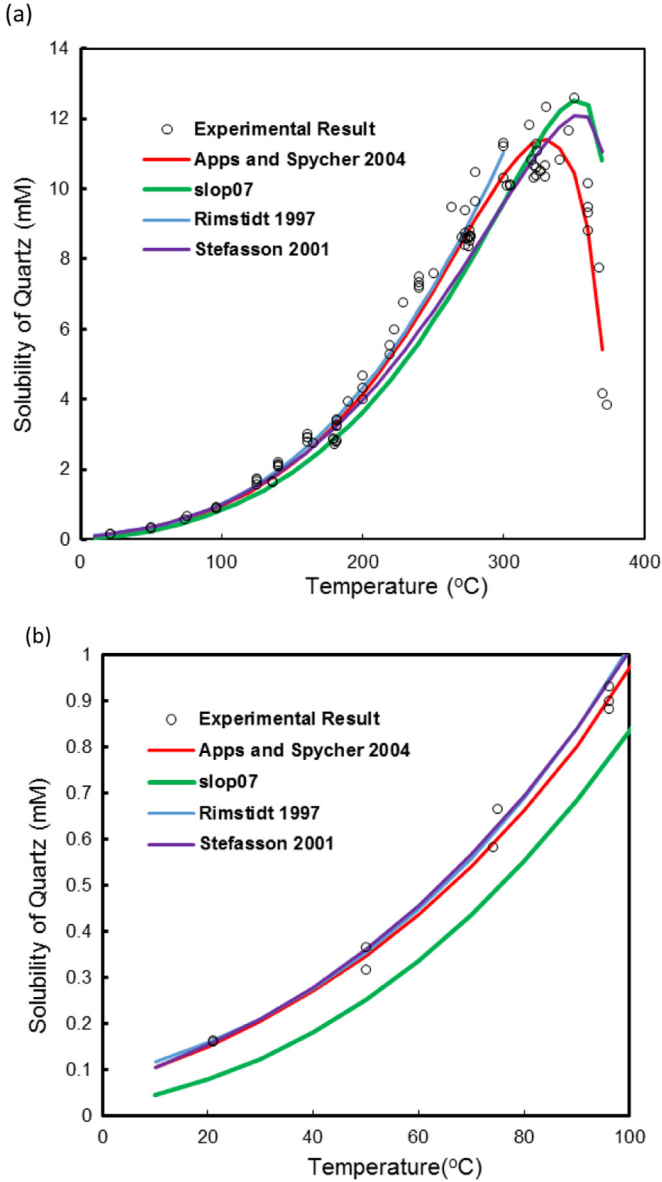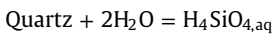
(a)

(b)

Fig. 6. Comparison between quartz solubility experimental data measured and compiled by Rimstidt (1997) (Black circles) and calculated results using SUPCRTBL and SUPCRT92. Rimstidt (1997) (Blue line): empirical Van't Hoff equation; slop07 (Green line): quartz from HDNB and SiO_2(aq) from Shock et al. (1997b); Stefansson (2001) (Purple line): quartz from HP11, $H_4SiO_4^\circ$(aq) from Stefansson (2001); Apps and Spycher 2004 (Red line): quartz from HP11 and SiO_2(aq) from Apps and Spycher (2004). (b) is an enlargement of (a) at low temperature. (b) Includes experimental data from Rimstidt (1997) only. (For interpretation of the references to color in this figure legend, the reader is referred to the web version of this article.)

Fig. 7. SUPCRTBL calculated molar volume of stishovite at 298.15 K as a function of pressure (blue dashed line), which was overlain onto HP11 Fig. 4 (black solid line). Squares and circles are experimental data reported by HP11. (For interpretation of the references to color in this figure legend, the reader is referred to the web version of this article.)
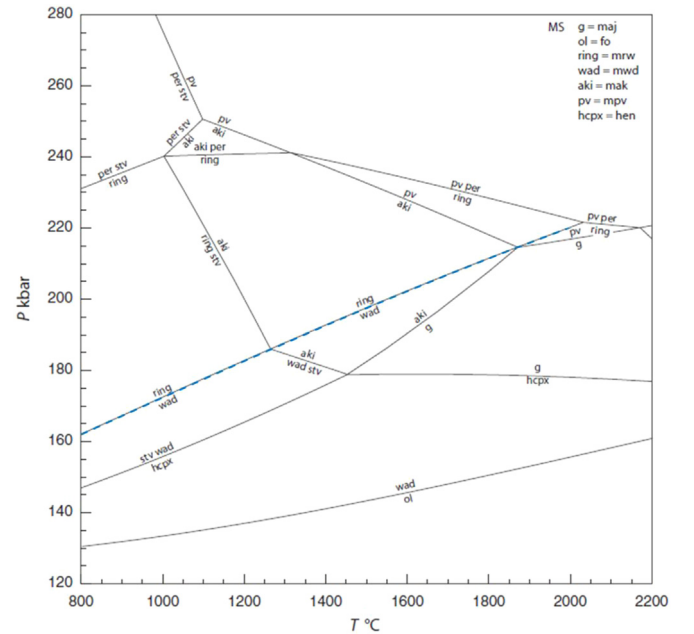
Fig. 8. SUPCRTBL calculated phase boundary between Mg-ringwoodite and Mg-wadsleyite as a function of temperature and pressure (blue dashed line), which is overlain onto HP11 Fig 9 (black lines). (For interpretation of the references to color in this figure legend, the reader is referred to the web version of this article.)

Gibbs free energy of formation and entropy for SiO_2(aq). From the solubility data, Rimstidt (1997) used standard thermodynamic properties for quartz and water from Robie and Hemingway (1995) to derive the standard thermodynamic properties for $H_4SiO_4^\circ$(aq).

$$Quartz + 2H_2O = H_4SiO_{4,aq}$$

The log K of this reaction was calculated using this updated SUPCRTBL, and then was converted to quartz solubility based on the following equation, which is valid at low ionic strength solution.

$$\log K = \log\left(\frac{a_{SiO_2,aq}}{a_{Quartz}}\right) = \log\left(\frac{m_{SiO_2,aq}}{1}\right) = \log m_{SiO_2,aq} \quad (12)$$

where K is the equilibrium constant, a_i is the activity of species i, m_i is the molality of species i (mol/kg). $a_{SiO_2,aq} = \sim m_{SiO_2,aq}$ in low salinity solution, and a_{Quartz} is 1.

The thermodynamic properties of aqueous silica (SiO_2,aq) (enthalpy and entropy) and HKF parameters c_1, c_2, and ω are fitted by Apps and Spycher (2004) using HKF model based on the experimental data that Rimstidt (1997) compiled. Four HKF volume parameters a_1–a_4 are from slop07.dat. Stefansson (2001) also evaluated the quartz and amorphous silica solubility data and derived standard molal properties and HKF parameters for $H_4SiO_4^\circ$(aq), which is an alternate form expressing dissolved silica. We decide to keep both in our database, and let the users to decide which one to use.

With these values, we calculated the solubility of quartz at 10–370 °C with various datasets, and compare them with the experimental data evaluated by Rimstidt (1997). Fig. 6 shows the

Table 4

Comparison of updates of thermodynamic properties of aqueous and mineral species from SUPCRT92.dat database.

	SUPCRT96.dat	SLOP98.dat	SLOP07.dat	SUPCRTBL.dat
Aqueous Species	Al-bearing species and NaOH° from Pokrovskii and Helgeson (1995)	Al-bearing species, from Shock et al. (1997b)	Al-bearing species, from Shock et al. (1997b)	Al-bearing species from Tagirov and Schott (2001)
	Metal–organic complexes and other organic compounds from Shock (1992,·1993), Shock and Koretsky (1993,·1995), Shock and McKinnon (1993), Schulte and Shock (1993), Haas et al. (1995), and references therein	Metal–organic complexes and other organic compounds from Shock (1992,·1993), Shock and Koretsky (1993,·1995), Shock and McKinnon (1993), Schulte and Shock (1993), Haas et al. (1995), and references therein	Metal–organic complexes and other organic compounds from Shock (1992,1993, 1995, 2009), Shock and Koretsky (1993,·1995), Shock and McKinnon (1993), Schulte and Shock (1993), Haas et al. (1995), Dale et al. (1997), Haas and Shock (1999), Prapaipong et al. (1999), Amend and Shock (2001), Amend and Plyasunov (2001), Plyasunov and Shock (2001), Schulte and Rogers (2004), Dick et al. (2006), LaRowe and Helgeson (2006a, 2006b) and references therein	Metal–organic complexes and other organic compounds from Shock (1992, 1993, 1995), Shock and Koretsky (1993,·1995), Shock and McKinnon (1993), Schulte and Shock (1993), Haas et al. (1995), Dale et al. (1997) and references therein
	Palladium from Sassani and Shock (1998)	Uranium from Shock et al. (1997a); Platinum-Group from Sassani and Shock (1998).	Uranium from Shock et al. (1997a); Platinum-Group from Sassani and Shock (1998); Actinides from Murphy and Shock (1999).	Uranium from Shock et al. (1997a); Platinum-Group from Sassani and Shock (1998). SiO_2° and $HSiO_3^-$ from Apps and Spycher (2004), Rimstidt (1997) and Stefansson (2001) As-bearing species from Nordstrom and Archer (2002). Metal–arsenate and metal–arsenite aqueous complexes from Marini and Accornero (2010)
Minerals	All other species from Sverjensky et al. (1997) and those internally consistent to Sverjensky et al. (1997)in earlier Helgeson and co-workers' publications Al oxyhydroxides from Pokrovskii and Helgeson (1995); all others from Helgeson et al. (1978)	All other species from Sverjensky et al. (1997) and those internally consistent to Sverjensky et al. (1997) in earlier Helgeson and co-workers' publications Helgeson et al. (1978)	All other species from Sverjensky et al. (1997) and those internally consistent to Sverjensky et al. (1997) in earlier Helgeson and co-workers' publications Helgeson et al. (1978)	All other species from Sverjensky et al. (1997) and those internally consistent to Sverjensky et al. (1997) in earlier Helgeson and co-workers' publications Holland and Powell (2011); Boehmite from Hemingway et al. (1991); Gibbsite from Robie et al. (1978); Dawsonite from this study; Arsenopyrite from Ball and Nordstrom (1991); Scorodite and Ferric-As,am from Langmuir et al. (2006); Barium–As and Barium–H–As from Zhu et al. (2005); all other As-bearing solids from Nordstrom and Archer (2002)

experimental data compiled by Rimstidt (1997) and the calculated values using the updated SUPCRTBL as well as results using slop07. dat and other models for comparison.

To verify the volume calculations in SUPCRTBL, we compared calculated stishovite molal volume as a function of pressure up to 2000 kbars to those in HP 11 in Fig. 7. Our calculated values overlap with those calculations in HP 11's (Fig. 4). To verify the Gibbs free energy calculations, we calculated the univariant phase boundary for Mg-ringwoodite and Mg-wadsleyite in the temperature range of 800–1800 °C and pressure range of 160 to ~200 kbars. Our calculated values overlap with those in HP 11 (Fig. 8)

6. Conclusions and remarks

There is little doubt that the development of SUPCRT92 software package and affiliated thermodynamic datasets has greatly contributed for making geochemical calculations highly efficient and improving our understanding of geochemical systems. Built on these successes, we have modified the dataset for SUPCRT92. The thermodynamic properties of some aqueous species and minerals have been updated, which include Al-bearing aqueous and mineral phases, As-bearing aqueous and mineral phases, $SiO_2^\circ(aq)$, $HSiO_3^-$ and dawsonite. The modifications are in line with new needs and interests of metamorphic petrology, economic geology, arsenic geochemistry, and carbon management. Table 4 compares the updates from this study with previous efforts of updating slop98.dat.

There are still many limitations and uncertainties with this dataset, however. The development of thermodynamic databases for the modeling of geochemical processes is an ongoing process. We need to continuously identify species with incorrect information and develop new equations and algorithms. Because of this need, we are compiling a relational database in order to make update thermodynamic data and the program easier. The program, dataset, updates, and corrections can be found at www.indiana.edu/~hydrogeo/supcrtbl.html.

Acknowledgments

Appendix A. Implementation of Holland and Powell's phase transition and order–disorder

In order to adopt HP's treatment of phase transitions and order-disorder in minerals into SUPCRT, the following equations were programmed in the code. For the minerals listed in Table 2b of HP11, T_c°, S_{max}, V_{max} values are included in our revised database. HP11 treats order-disorder transitions in solid solutions with a macroscopic Bragg–Williams type of model (Table 2c of HP11). However, complete

documentation of this treatment is not yet publically available for programming into SUPCRT. In the current SUPCRTBL code and accompanying database, we used the Landau model and parameters in HP98 for the minerals in Table 2c of HP11. However, those minerals in Table 2c that do not have Landau parameters in HP98 currently do not have phase transition provisions available in SUPCRTBL.

Landau theory

Landau theory is an empirical way to describe how the thermodynamic properties change with the order-disorder structure of minerals. It provides a more precise way to calculate the thermodynamic properties of minerals near phase transition temperature, especially heat capacity (Fig. 1, A1, A2 and A3). The incorporation of HP11 thermodynamic data for minerals makes it necessary to modify SUPCRT92 to use tricritical Landau model to predict the thermodynamic properties of minerals.

Calculation of thermodynamic properties using Landau theory

All equations below are from HP90 and HP98. Phase transition temperature at given pressure is described as:

$$T_C = T_C^\circ + \frac{V_{max}}{S_{max}}P \tag{A.1}$$

where T_C is the critical temperature (K) at a given pressure, T_C° is the critical temperature at 1 bar (K), V_{max} is the volume of disordering at T_C° (J/bar), S_{max} is the entropy of disordering at T_C° (kJ/mol/K), and P is the pressure of interest (kbar).

Calculation of order parameter (Q)

$$Q = \begin{cases} \left(\dfrac{T_C - T}{T_C^\circ}\right)^{0.25} & (T \leq T_C) \\ 0 & (T > T_C) \end{cases}$$

$$Q_0 = \left(\frac{T_C^\circ - 298.15K}{T_C^\circ}\right) \tag{A.2}$$

where Q is the order parameter, which is a dimensionless number that describes the order-disorder structure of minerals. $Q=1$ means the structure is completely ordered, and $Q=0$ means the structure is completely disordered. Q_0 is the order parameter at 298.15 K and 1 bar. T is temperature of interest (K).

Calculation of excess values of thermodynamic properties

$$C_p^{ex} = \begin{cases} \dfrac{S_{max}T}{2\sqrt{T_C}\sqrt{T_C - T}} & (T \leq T_C) \\ 0 & (T > T_C) \end{cases} \tag{A.3}$$

$$V^{ex} = V_{max}\left(1 - Q_0^2\right) \tag{A.4}$$

$$H^{ex} = 2S_{max}T_c\left(\frac{Q^6}{6} - \frac{Q^2}{2} + \frac{1}{3}\right) \tag{A.5}$$
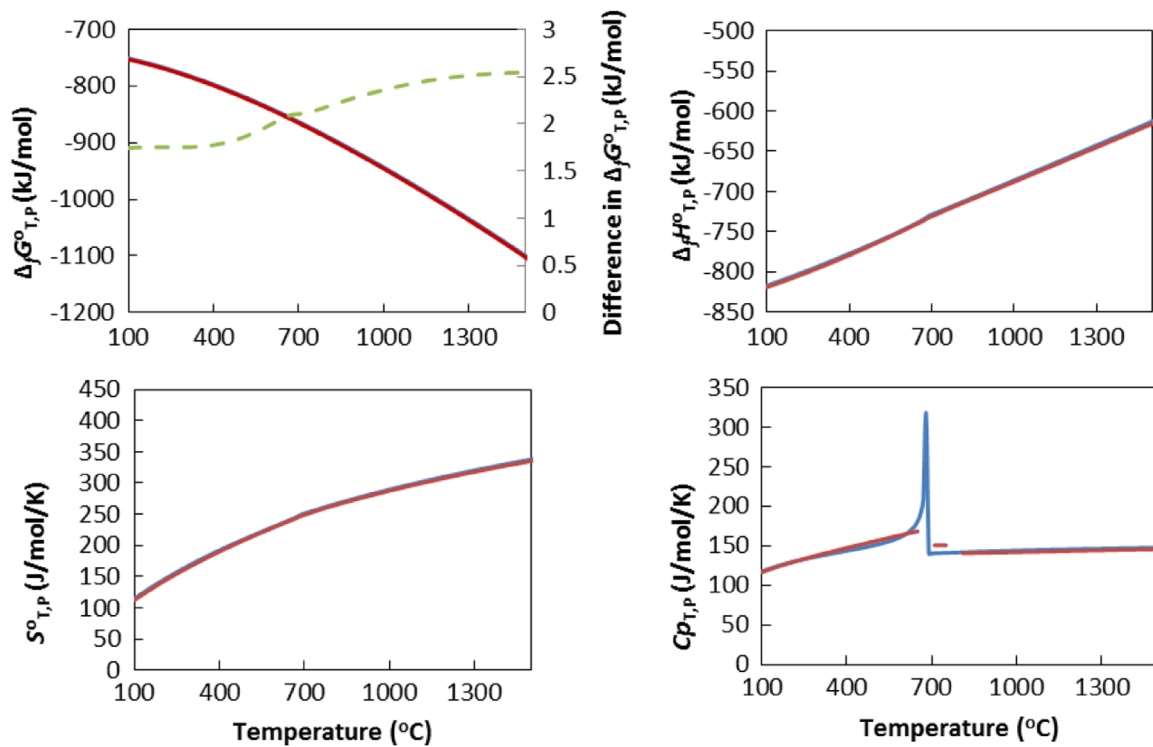
Fig. A1. Comparison of thermodynamic properties of hematite as a function of temperature at 1 bar between SUPCRT92 (red line) and SUPCRTBL (blue line). The difference in $\Delta_f G^\circ_{T,P}$ is shown with green dashed line.
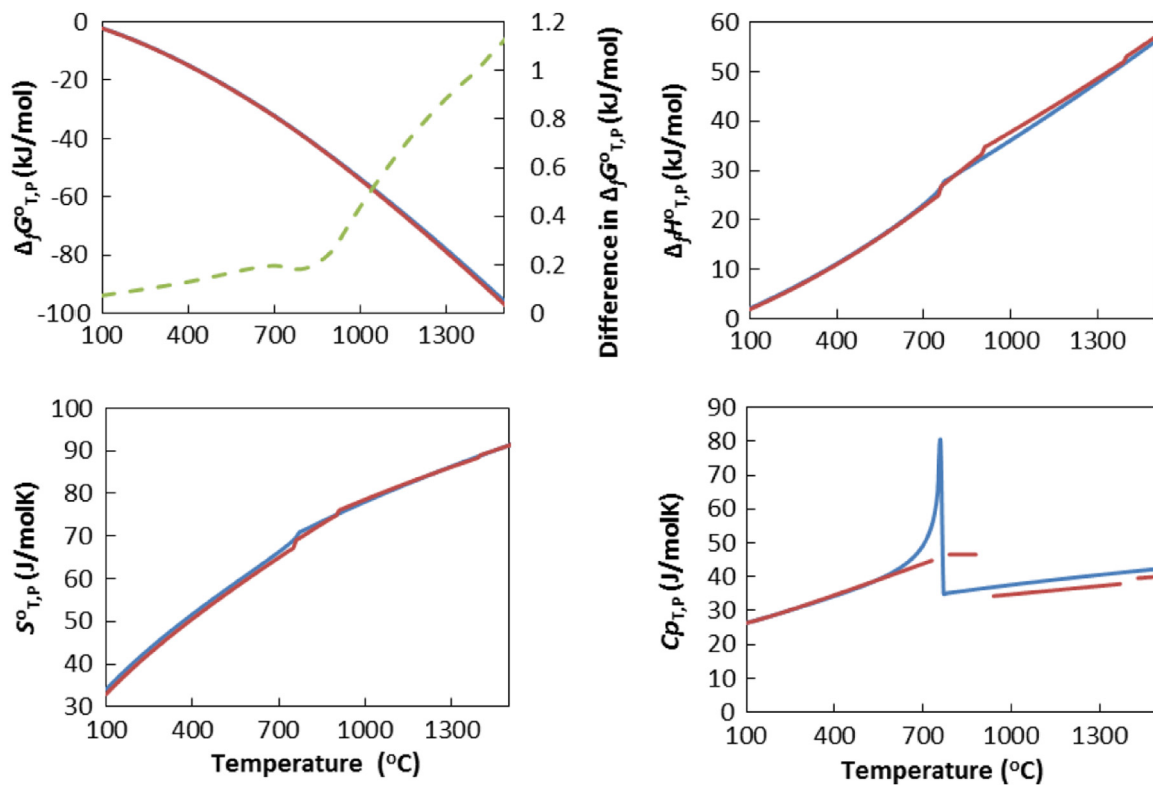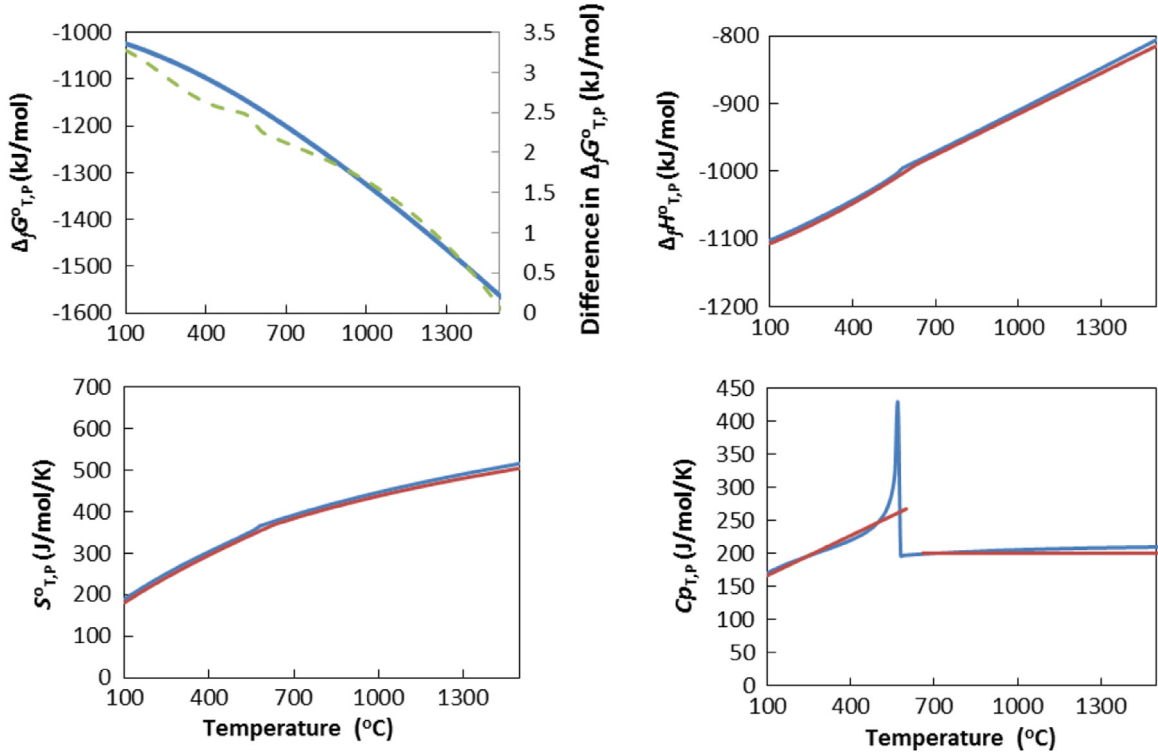

Fig. A2. Comparison of thermodynamic properties of iron as a function of temperature at 1 bar between SUPCRT92 (red line) and SUPCRTBL (blue line). The difference in $\Delta_f G^\circ_{T,P}$ is shown with green dashed line.

Fig. A3. Comparison of thermodynamic properties of magnetite as a function of temperature at 1 bar between SUPCRT92 (red line) and SUPCRTBL (blue line). The difference in $\Delta_f G^\circ_{T,P}$ is shown with green dashed line.

$$S^{ex} = S_{max}\left(1 - Q^2\right) \tag{A.6}$$

$$G^{ex} = T_C^\circ S_{max}\left(Q_0^2 - \frac{1}{3}Q_0^6\right) - S_{max}\left(T_C Q^2 - \frac{1}{3}T_C^\circ Q^6\right)$$
$$- TS_{max}\left(Q_0^2 - Q^2\right) + \int v_T^{\cdot} dP \tag{A.7}$$

where Cp^{ex}, V^{ex}, H^{ex}, S^{ex}, and G^{ex} are the excess heat capacity, molar volume, enthalpy, entropy, and Gibbs free energy of disordering at T and P of interest (kJ/mol/K, kJ/kbar, kJ/mol, kJ/mol/K, and kJ/mol respectively). The last term in Eq. (A.7) accounts for the contribution of excess molar volume to excess Gibbs free energy. The expression of this term can be found in Eqs. (A.8) and (A.9)

$$\int v_T^{\cdot} dP = \frac{1}{3}V_{max} Q_{298}^2\left(1 + \alpha^\circ(T - T_r) - 20\alpha^\circ\left(\sqrt{T} - \sqrt{T_r}\right)\right)\kappa_T$$
$$\left(\left(1 + \frac{4P}{\kappa_T}\right)^{3/4} - 1\right) \tag{A.8}$$

$$\kappa_T = \kappa^\circ\left(1 - 1.5 \times 10^{-4}(T - T_r)\right) \tag{A.9}$$

where α° is the thermal expansivity of the mineral (K^{-1}) at 298.15 K and 1 bar, and κ_T is the bulk modulus of the mineral (kbar) at T of interest and 1 bar. κ° is the bulk modulus (kbar) at 298.15 K and 1 bar. T_r is reference temperature which equals 298.15 K.

Calculation of thermodynamic properties at given T and P

The thermodynamic properties at given T and P can be found

by adding the excess terms in Eqs. (A.3–A.7) to the calculated properties without considering phase transition (thermodynamic properties of hypothetical ordered form of that mineral at given T and P).

References

Amend, J.P., Plyasunov, A.V., 2001. Carbohydrates in thermophile metabolism: calculation of the standard molal thermodynamic properties of aqueous pentoses and hexoses at elevated temperatures and pressures. Geochim. Et. Cosmochim. Acta 65, 3901–3917.

Amend, J.P., Shock, E.L., 2001. Energetics of overall metabolic reactions of thermophilic and hyperthermophilic Archaea and Bacteria. FEMS Microbiol. Rev. 25, 175–243.

Anderson, G.M., 2008. Thermodynamics of Natural Systems. Cambridge University Press, United Kingdom.

Andre, L., Audigane, P., Azaroual, M., Menjoz, A., 2007. Numerical modeling of fluid–rock chemical interactions at the supercritical CO_2–liquid interface during CO_2 injection into a carbonate reservoir, the Dogger aquifer (Paris Basin, France). Energy Convers. Manag. 48, 1782–1797.

Apps J. and Spycher N. (2004) Data Qualification for Thermodynamic Data Used to Support THC Calculations. ANL-NBS-HS-000043 REV 00, Bechtel SAIC Company, LLC, Las Vegas, NV. 172 pp. DOC.20041118.0004.

Bachu, S., 2008. CO_2 storage in geological media: role, means, status and barriers to deployment. Prog. Energy Combust. Sci. 34, 254–273.

Ball, J.W., Nordstrom, D.K., 1991. User's Manual for WATEQ4F, with Revised Thermodynamic Data Base and Test Cases for Calculating Speciation of Major, Trace, and Redox Elements in Natural Waters, pp. 91–183, U.S.Geological Survey Open File Report.

Benezeth, P., Palmer, D.A., Anovitz, L.M., Horita, J., 2007. Dawsonite synthesis and reevaluation of its thermodynamic properties from solubility measurements: implications for mineral trapping of CO_2. Geochim. Et. Cosmochim. Acta 71, 4438–4455.

Berman, R.G., 1988. Internally-consistent thermodynamic data for minerals in the system Na_2O–K_2O–CaO–MgO–FeO–Fe_2O_3–Al_2O_3–SiO_2–TiO_2–H_2O–CO_2. J. Petrol. 29, 445–522.

Cox, J., Wagman, D.D., Medvedev, V.A., 1989. CODATA Key Values for Thermodynamics. Hemisphere Publishing Corp, New York.

Dale, J.D., Shock, E.L., Macleod, G., Aplin, A.C., Larter, S.R., 1997. Standard partial molal properties of aqueous alkylphenols at high pressures and temperatures. Geochim. Et. Cosmochim. Acta 61, 4017–4024.

Dick, J., LaRowe, D., Helgeson, H., 2006. Temperature, pressure, and electrochemical

constraints on protein speciation: group additivity calculation of the standard molal thermodynamic properties of ionized unfolded proteins. Biogeosciences 3, 311–336.

Ferrante, M.J., Stuve, J.M., Richardson, D.W., 1976. Thermodynamic data for synthetic dawsonite. U. S. Bureau of Mines Report of Investigations No. 8129, 13 pp.

Freund, J., Ingalls, R., 1989. Inverted isothermal equations of state and determination of B_0, B'_0 and B''_0. J. Phys. Chem. Solids 50, 263–268.

Fukushi, K., Sverjensky, D.A., 2007. A predictive model (ETLM) for arsenate adsorption and surface speciation on oxides consistent with spectroscopic and theoretical molecular evidence. Geochim. Et. Cosmochim. Acta 71, 3717–3745.

Geopig (2010) Available at: http://geopig.asu.edu/ [Accessed February 19, 2016].

Gunnarsson, I., Arnórsson, S., 2000. Amorphous silica solubility and the thermodynamic properties of $H_4SiO_4^0$ in the range of 0° to 350 °C at P_{sat}. Geochim. Et. Cosmochim. Acta 64, 2295–2307.

Haas, J.R., Shock, E.L., 1999. Halocarbons in the environment: estimates of thermodynamic properties for aqueous chloroethylene species and their stabilities in natural settings. Geochim. Et. Cosmochim. Acta 63, 3429–3441.

Haas, J.R., Shock, E.L., Sassani, D.C., 1995. Rare earth elements in hydrothermal systems: estimates of standard partial molal thermodynamic properties of aqueous complexes of the rare earth elements at high pressures and temperatures. Geochim. Et. Cosmochim. Acta 59, 4329–4350.

Helgeson, H.C., Delany, J.M., Nesbitt, H.W., Bird, D.K., 1978. Summary and critique of the thermodynamic properties of rock forming minerals. Am. J. Sci. 278A, 569–592.

Hemingway, B., Robie, R., Fisher, J., Wilson, W., 1977. Heat capacities of gibbsite, Al(OH)$_3$, between 13 and 480 K and magnesite, MgCO$_3$, between 13 and 380 K and their standard entropies at 289.15 K, and the heat capacities of calorimetry conference benzoic acid between 12 and 316 K. J. Res. US Geol. Surv., 5.

Hemingway, B.S., Robie, R.A., Kittrick, J.A., 1978. Revised values for the Gibbs free energy of formation of $Al(OH)_4aq-$, diaspore, boehmite and bayerite at 298.15 K and 1 bar, the thermodynamic properties of kaolinite to 800 K and 1 bar, and the heats of solution of several gibbsite samples. Geochim. Et. Cosmochim. Acta 42, 1533–1543.

Hemingway, B.S., Robie, R.A., Apps, J.A., 1991. Revised values for the thermodynamic properties of boehmite, AlO(OH), and related species and phases in the system Al–H–O. Am. Mineral., 445–457.

Holland, T., Carpenter, M., 1986. Aluminium/silicon disordering and melting in sillimanite at high pressures. Nature 320, 151–153.

Holland, T., Powell, R., 2011. An improved and extended internally consistent thermodynamic dataset for phases of petrological interest, involving a new equation of state for solids. J. Metamorph. Geol. 29, 333–383.

Holland, T., Redfern, S.A., Pawley, A., 1996. Volume behavior of hydrous minerals at high pressure and temperature: II. Compressibilities of lawsonite, zoisite, clinozoisite, and epidote. Am. Mineral. 81, 341–348.

IPCC, 2005. Special report: carbon dioxide capture and storage. In: Metz, B., Davidson, O., de Coninck, H., Loos, M., Meyer, L. (Eds.), Cambridge Univ Press, Cambridge, UK.

Johnson, J.W., Oelkers, E.H., Helgeson, H.C., 1992. SUPCRT92-A software package for calculating the standard molal thermodynamic properties of minerals, gases, aqueous species, and reactions from 1-bar to 5000-bar and 0 °C to 1000 °C. Comput. Geosci. 18, 899–947.

Johnson, J.W., Nitao, J.J., Knauss, K.G., 2004. Reactive transport modeling of CO$_2$ storage in saline aquifers to elucidate fundamental processes, trapping mechanisms, and sequestration partitioning. In: Baines, S.J., Worden, R.H. (Eds.), Geologic Storage of Carbon Dioxide, Geological Society, London, pp. 107–128.

Langmuir, D., Mahoney, J., Rowson, J., 2006. Solubility products of amorphous ferric arsenate and crystalline scorodite (FeAsO$_4 \cdot 2H_2O$) and their application to arsenic behavior in buried mine tailings. Geochim. Cosmochim. Acta 70, 2942–2956.

LaRowe, D.E., Helgeson, H.C., 2006a. Biomolecules in hydrothermal systems: calculation of the standard molal thermodynamic properties of nucleic-acid bases, nucleosides, and nucleotides at elevated temperatures and pressures. Geochim. Et. Cosmochim. Acta 70, 4680–4724.

LaRowe, D.E., Helgeson, H.C., 2006b. The energetics of metabolism in hydrothermal systems: calculation of the standard molal thermodynamic properties of magnesium-complexed adenosine nucleotides and NAD and NADP at elevated temperatures and pressures. Thermochim. Acta 448, 82–106.

Liu, F.Y., Lu, P., Zhu, C., Xiao, Y., 2011. Coupled reactive transport modeling of CO$_2$ Sequestration in the Mt. Simon Sandstone Formation, Midwest U.S.A. Int. J. Greenh. Gas Control 52, 297–307.

Lu, P., Zhu, C., 2011. Arsenic Eh–pH diagrams at 25 °C and 1 bar. Environ. Earth Sci. 62, 1673–1683.

Maier, C.G., Kelley, K., 1932. An equation for the representation of high-temperature heat content data1. J. Am. Chem. Soc. 54, 3243–3246.

Marini, L., Accornero, M., 2007. Prediction of the thermodynamic properties of metal–arsenate and metal–arsenite aqueous complexes to high temperatures and pressures and some geological consequences. Environ. Geol. 52, 1343–1363.

Marini, L., Accornero, M., 2010. Prediction of the thermodynamic properties of metal–arsenate and metal–arsenite aqueous complexes to high temperatures and pressures and some geological consequences. Environ. Earth Sci. 59, 1601–1606.

McKnight-Whitford, A., Chen, B.W., Naranmandura, H., Zhu, C., Le, X.C., 2010. New method and detection of high concentrations of monomethylarsonous acid detected in contaminated groundwater. Environ. Sci. Technol. 44, 5875–5880.

Murphy, W.M., Shock, E.L., 1999. Environmental aqueous geochemistry of actinides.

Reviews in Mineralogy 38, 221–253.

Nordstrom, D.K., Archer, D.G., 2002. Arsenic thermodynamic data and environmental geochemistry. In: Welch, A.H., Stollenwerk, K.G. (Eds.), Arsenic in Ground Water. Springer, US, Boston, MA.

Oelkers, E.H., Bénézeth, P., Pokrovski, G.S., 2009. Thermodynamic databases for water–rock interaction. Rev. Miner. Geochem. 70, 1–46.

Oremland, R.S., Stolz, J.F., 2003. The ecology of Arsenic. Science 300, 939–944.

Pawley, A., Redfern, S.A., Holland, T., 1996. Volume behavior of hydrous minerals at high pressure and temperature: I. Thermal expansion of lawsonite, zoisite, clinozoisite, and diaspore. Am. Mineral. 81, 335–340.

Plyasunov, A.V., Shock, E.L., 2001. Correlation strategy for determining the parameters of the revised Helgeson–Kirkham–Flowers model for aqueous nonelectrolytes. Geochim. Et. Cosmochim. Acta 65, 3879–3900.

Pokrovski, G.S., Kara, S., Roux, J., 2002. Stability and solubility of arsenopyrite, FeAsS, in crustal fluids. Geochim. Cosmochim. Acta 66, 2361–2378.

Pokrovskii, V.A., Helgeson, H.C., 1995. Thermodynamic properties of aqueous species and the solubilities of minerals at high pressures and temperatures: the system Al$_2$O$_3$–H$_2$O–NaCl. Am. J. Sci. 295, 1255–1342.

Prapaipong, P., Shock, E.L., Koretsky, C.M., 1999. Metal–organic complexes in geochemical processes: temperature dependence of the standard thermodynamic properties of aqueous complexes between metal cations and dicarboxylate ligands. Geochim. Et. Cosmochim. Acta 63, 2547–2577.

Rimstidt, J.D., 1997. Quartz solubility at low temperatures. Geochim. Et. Cosmochim. Acta 61, 2553–2558.

Robie, R.A., Hemingway, B.S., 1995. Thermodynamic properties of minerals and related substances at 298.15 K and 1 bar (10^5 Pa) pressure and at higher temperatures. U.S. Geol. Surv. Bull. 2131, 456.

Robie, R.A., Hemingway, B.S., Fisher, J.R., 1978. Thermodynamic properties of minerals and related substances at 298.15 K and 1 bar (105 Pa) pressure and at higher temperatures. U.S. Geol. Surv. Bull. 1452, 456.

Sassani, D.C., Shock, E.L., 1998. Solubility and transport of platinum-group elements in supercritical fluids: summary and estimates of thermodynamic properties for ruthenium, rhodium, palladium, and platinum solids, aqueous ions, and complexes to 1000 °C and 5 kbar. Geochim. Et. Cosmochim. Acta 62, 2643–2671.

Schulte, M.D., Shock, E.L., 1993. Aldehydes in hydrothermal solution: standard partial molal thermodynamic properties and relative stabilities at high temperatures and pressures. Geochim. Et. Cosmochim. acta 57, 3835–3846.

Schulte, M.D., Rogers, K.L., 2004. Thiols in hydrothermal solution: standard partial molal properties and their role in the organic geochemistry of hydrothermal environments. Geochim. Et. Cosmochim. Acta 68, 1087–1097.

Shock, E.L., 1992. Stability of peptides in high-temperature aqueous solutions. Geochim. Et. Cosmochim. acta 56, 3481–3491.

Shock, E.L., 1993. Hydrothermal dehydration of aqueous organic compounds. Geochim. Et. Cosmochim. acta 57, 3341–3349.

Shock, E.L., 1995. Organic acids in hydrothermal solutions: standard molal thermodynamic properties of carboxylic acids and estimates of dissociation constants at high temperatures and pressures. Am. J. Sci. 295, 496–580.

Shock, E.L., 2009. Minerals as energy sources for microorganisms. Econ. Geol. 104, 1235–1248.

Shock, E.L., Koretsky, C.M., 1993. Metal–organic complexes in geochemical processes: calculation of standard partial molal thermodynamic properties of aqueous acetate complexes at high pressures and temperatures. Geochim. Et. Cosmochim. Acta 57, 4899–4922.

Shock, E.L., McKinnon, W.B., 1993. Hydrothermal processing of cometary volatiles—applications to Triton. Icarus 106, 464–477.

Shock, E.L., Koretsky, C.M., 1995. Metal–organic complexes in geochemical processes-estimation of standard partial molal thermodynamic properties of aqueous complexes between metal-cations and monovalent organic-acid ligands at high-pressures and temperatures. Geochim. Et. Cosmochim. Acta 59, 1497–1532.

Shock, E.L., Sassani, D.C., Betz, H., 1997a. Uranium in geologic fluids: estimates of standard partial molal properties, oxidation potentials, and hydrolysis constants at high temperatures and pressures. Geochim. Et. Cosmochim. Acta 61, 4245–4266.

Shock, E.L., Sassani, D.C., Willis, M., Sverjensky, D.A., 1997b. Inorganic species in geologic fluids: correlations among standard molal thermodynamic properties of aqueous ions and hydroxide complexes. Geochim. Et. Cosmochim. Acta 61, 907–950.

Smedley, P.L., Kinniburgh, D.G., 2002. A review of the source, behaviour and distrbution of arsenic in natural waters. Appl. Geochem. 17, 517–568.

Stefansson, A., 2001. Dissolution of primary minerals of basalt in natural waters: I. Calculation of mineral solubilities from 0 °C to 350 °C. Chem. Geol. 172, 225–250.

Strazisar, B.R., Zhu, C., Hedges, S.W., 2006. Preliminary modeling of the long-term fate of CO$_2$ following injection into deep geological formations. Environ. Geosci. 13, 1–15.

Sverjensky, D.A., Fukushi, K., 2006. A predictive model (ETLM) for As(III) adsorption and surface speciation on oxides consistent with spectroscopic data. Geochim. Et. Cosmochim. Acta 70, 3778–3802.

Sverjensky, D.A., Shock, E.L., Helgeson, H.C., 1997. Prediction of the thermodynamic properties of aqueous metal complexes to 5 Kb and 1000 °C. Geochim. Et. Cosmochim. Acta 61, 1359–1412.

Swartz, C.H., Blute, N.K., Badruzzman, B., Ali, A., Brabander, D., Jay, J., Besancon, J., Islam, S., Hemond, H.F., Harvey, C.F., 2004. Mobility of arsenic in a Bangladesh aquifer: inferences from geochemical profiles, leaching data, and mineralogical

characterization. Geochim. Cosmochim. Acta 68, 4539–4557.

Tagirov, B., Schott, J., 2001. Aluminum speciation in crustal fluids revisited. Geochim. Et. Cosmochim. Acta 65, 3965–3992.

Tutolo, B.M., Kong, X.-Z., Seyfried Jr, W.E., Saar, M.O., 2014. Internal consistency in aqueous geochemical data revisited: applications to the aluminum system. Geochim. Et. Cosmochim. Acta 133, 216–234.

Wagman, D.D., Evans, W.H., Parker, V.B., Schumm, R.H., Halow, I., Bailey, S.M., Churney, K.L., Nuttall, R.L., 1982. The NBS tables of chemical thermodynamic properties-selected values for inorganic and C-1 and C-2 organic-substances in SI units. J. Phys. Chem. Ref. Data 11 (Suppl 2), S392.

Welch, A.H., Westjohn, D.B., Helsel, D.R., Wanty, R.B., 2000. Arsenic in ground water of the United States: occurence and geochemistry. Ground Water 38, 589–604.

Wesolowski, D.J., 1992. Aluminum speciation and equilibria in aqueous-solution.1. The solubility of Gibbsite in the system Na–K–Cl–OH–Al(OH)$_4$ from 0° to 100 °C. Geochim. Et. Cosmochim. Acta 56, 1065–1091.

Xu, T., Apps, J.A., Pruess, K., 2004. Numerical simulation of CO_2 disposal by mineral trapping in deep aquifers. Appl. Geochem. 19, 917–936.

Zhang, G.R., Lu, P., Zhang, Y.L., Wei, X.M., Zhu, C., 2015. Effects of rate law formulation on predicting CO_2 sequestration in sandstone formations. Int. J. Energy Res. 39, 1890–1908.

Zhu, C., Lu, P., 2009. Alkali feldspar dissolution and secondary mineral precipitation in batch systems: 3. Saturation states of product minerals and reaction paths. Geochim. Et. Cosmochim. Acta 73, 3171–3200.

Zhu, Y., Zhang, X., Xie, Q., Chen, Y., Wang, D., Liang, Y., Lu, J., 2005. Solubility and stability of barium arsenate and barium hydrogen arsenate at 25 °C. J. Hazard. Mater. 120, 37–44.

Zhu, C., Zhang, G., Lu, P., Meng, L., Ji, X., 2015. Benchmark modeling of the Sleipner CO2 plume: calibration to seismic data for the uppermost layer and model sensitivity analysis. Int. J. Greenh. Gas Control 43, 233–246.